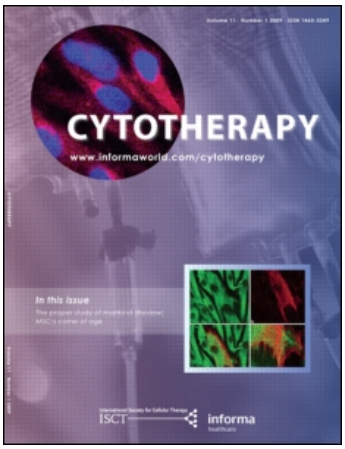

Cytotherapy
Publication details, including instructions for authors and subscription information:
http://www.informaworld.com/smpp/title~content=t713656803

Analysis of changes in the viability and gene expression profiles of human mesenchymal stromal cells over time

Kyoung A. Lee [a]; Wooyoung Shim [ab]; Man Jeong Paik [b]; Soo Cheol Lee [a]; Jin Young Shin [bc]; Young Hwan Ahn [bc]; Kiho Park [d]; Jeong Hyun Kim [a]; Sangdun Choi [a]; Gwang Lee [abe]
[a] Department of Molecular Science and Technology, Ajou University, Suwon, South Korea [b] Institute for Neuroregeneration and Stem Cell Research, Ajou University School of Medicine, Suwon, South Korea [c] Department of Neurosurgery, ajou University School of Medicine, Suwon, South Korea [d] Department of Pediatrics, Wallace Memorial Baptist Hospital, Pusan, South Korea [e] Institute for Medical Science, Ajou University School of Medicine, Suwon, South Korea

Online Publication Date: 01 October 2009

To cite this Article Lee, Kyoung A., Shim, Wooyoung, Paik, Man Jeong, Lee, Soo Cheol, Shin, Jin Young, Ahn, Young Hwan, Park, Kiho, Kim, Jeong Hyun, Choi, Sangdun and Lee, Gwang(2009)'Analysis of changes in the viability and gene expression profiles of human mesenchymal stromal cells over time',Cytotherapy,11:6,688 — 697

To link to this Article: DOI: 10.3109/14653240902974032

URL: http://dx.doi.org/10.3109/14653240902974032

International Society for Cellular Therapy
ISCT

Cytotherapy (2009) Vol. 11, No. 6, 688–697

informa
healthcare

Analysis of changes in the viability and gene expression profiles of human mesenchymal stromal cells over time

Kyoung A. Lee[1], Wooyoung Shim[1,2], Man Jeong Paik[2], Soo Cheol Lee[1], Jin Young Shin[2,3], Young Hwan Ahn[2,3], Kiho Park[4], Jeong Hyun Kim[1], Sangdun Choi[a1] and Gwang Lee[1,2,5]

[1]Department of Molecular Science and Technology, Ajou University, Suwon, South Korea, [2]Institute for Neuroregeneration and Stem Cell Research, Ajou University School of Medicine, Suwon, South Korea, [3]Department of Neurosurgery, ajou University School of Medicine, Suwon, South Korea, [4]Department of Pediatrics, Wallace Memorial Baptist Hospital, Pusan, South Korea, and [5]Institute for Medical Science, Ajou University School of Medicine, Suwon, South Korea

Background aims

Because of their ability to differentiate and widespread availability, human mesenchymal stromal cells (hMSC) are often used as a clinical therapeutic tool. However, the factors that determine the quality and viability of hMSC are not well understood.

Methods

We evaluated the viability of hMSC over time using flow cytometry analysis (FACS) and transmission electron microscopy (TEM) to determine if morphologic changes occurred in hMSC. In addition, we conducted gene expression profiling using an Affymetrix Human Genome U133 Plus 2.0 Array.

Results

FACS analysis revealed that 83% and 76% of the cells were viable in sterilized phosphate-buffered saline (PBS) after 6 h and 12 h, respectively. TEM data revealed that the total number of cells with healthy chromatins or a few cytosolic vacuoles was significantly reduced over time. We then conducted gene expression profiling using a microarray, which revealed changes in the expression of 2949 functional genes. Specifically, among the total of 50 000 gene probes evaluated, the expression levels of apoptosis and stress-related genes were significantly increased over time.

Conclusions

The results of this study suggest that the viability of hMSC decreases after disassociation from the culture dish and time is an essential factor when considering hMSC as a potential source for stem cell-based direct transplantation.

Keywords

cell viability, human mesenchymal stromal cells, microarray, transplantation.

Introduction

Human mesenchymal stromal cells (hMSC) have been investigated for their efficacy as a clinical therapeutic tool in patients with stroke, myocardial infarction, limb ischemia and multiple system atrophy (MAS) [1–4] because of their availability and differentiation plasticity. hMSC have been isolated from a variety of tissues, including placenta, adipose tissue and bone marrow [5–8]. In addition, it is well known that MSC are multipotent and have the potential to differentiate into osteoblasts, chondroblasts, adipocytes and neurons both *in vitro* and *in vivo* [9–13], as well as the ability to support hematopoesis [14]. Furthermore, recent studies have shown that hMSC may be useful in tissue engineering [15].

It has been suggested that neurologic disorders can be treated by direct transplantation of stem cells or their derivatives into the adult brain [16]. We have reported previously that intravenous injection of *ex vivo*-cultured autologous hMSC into patients suffering from ischemic stroke and MAS had the potential to aid in their functional recovery [14]. In addition to being a safe and feasible method of

Correspondence to: **Gwang Lee**, PhD, Institute for Medical Sciences, Ajou University School of Medicine, San 5, Wonchon-dong, Yeongtong-gu, Suwon, 443–721, South Korea. E-mail: glee@ajou.ac.kr. Sangdum Choi, PhD, Department of Molecular Science and Technology, Ajou University, Suwon, 443–721, South Korea. E-mail: sangdunchoi@ajou.ac.kr

DOI: 10.3109/14653240902974032

treatment for brain diseases, there are no ethical problems associated with the use of autologous hMSC.

Li *et al.*17] reported that approximately 1–5% of transplanted hMSC express proteins that are phenotypic of brain parenchymal cells. Transplanted hMSC often have poor survival rates, which may occur as a result of mechanical trauma, free radicals, deprivation of growth factors and time following cell preparation [1819]. hMSC have a high potential for cell proliferation, differentiation and adhesion capacity immediately after harvest [20]. Although the viability of hMSC for transplantation has not been investigated thoroughly, it is well known that hMSC should be kept in a fresh condition by minimizing stress and damage prior to transplantation. Therefore, it is important to use hMSC as soon as possible following harvest to improve the chances of successful transplantation.

We conducted this study to analyze the viability and freshness of isolated hMSC that were stored in phosphate-buffered saline (PBS) prior to clinical applications. Although standard culture conditions and techniques have been developed to optimize the growth of hMSC, these conditions are inherently stressful to many other types of stem cells. Therefore, we evaluated changes in the viability and morphology of hMSC over time using flow fluorescence-activated cell sorting (FACS) and transmission electron microscopy (TEM) analysis, respectively. In addition, we utilized complementary (c)DNA microarray analysis to evaluate the effects of storage on the expression of genes by hMSC.

Methods

Cell culture

hMSC were obtained from 20-mL aspirates from the iliac crest of normal human donors [121]. The procedure used in this study was approved by the Scientific Ethical Review Board of Ajou University Medical Center (AJIRB-CRO-05-126; Suwon, South Korea). Briefly, human BM-derived MSC were aspirated from the human iliac crest and separated by 70% Percoll-gradient centrifugation. The cells in the low-density fraction were then washed with low-glucose Dulbecco's modified Eagle's medium (DMEM; Invitrogen, Calsbad, CA, USA) supplemented with 10% fetal bovine serum (FBS; Invitrogen) and antibiotics (100 U/mL penicillin and 100 mg/mL streptomycin sulfate; Invitrogen). Next, aliquots of 10^6 cells were seeded into 10-cm plastic culture dishes that contained control medium. The non-adherent cells were removed, after which the adherent cells were replated into new medium in 10-cm dishes and cultured at 37°C in a 5% CO_2 humidified atmosphere. After 24 h, cells that adhered to the pore-containing plate were recovered and plated again at a density of approximately 3×10^5 cells/mL. The samples were then incubated under the same conditions as described above until reaching a confluency of greater than 80%. Next, the cells were subcultured at a ratio of 1:3 for six passages using the aforementioned procedure. Approximately 1×10^6 cells from each fraction were centrifuged at 1200 r.p.m. for 3 min, washed three times in PBS and then incubated in PBS for various lengths of time (0, 3, 6 and 12 h).

Flow cytometry

Annexin V staining of exposed membrane phosphatidylserine was conducted using an Annexin VFITC apoptosis detection kit (BD Pharmigen, San Diego, CA, USA) according to the manufacturer's instructions. Briefly, cells were harvested and washed with 1×PBS twice, after which they were resuspended in 100 µL binding buffer (10 mm Hepes, pH 7.4, 140 mm sodium chloride and 2.5 mm calcium chloride). Annexin V–FITC and propidium iodide (PI) were then added to the individual samples, which were subsequently incubated for 15 min in a low-light environment. The reaction was stopped by adding an equal volume of binding buffer, after which the cells were analyzed by FACS (Facsvantage; Becton Dickinson, Franklin Lakes, NJ, USA).

TEM

Aliquots of the cell suspension were centrifuged at 4°C and 1000× **g** for 3 min, after which they were fixed with Karnovsky's fixative solution (1% paraformaldehyde, 2% glutaraldehyde, 2 mm calcium chloride and 100 mm cacodylate buffer, pH 7.4) for 1 day to 1 week. The cells were then washed with cacodylate buffer and post-fixed in 1% osmium tetroxide (OsO_4) containing 0.05% potassium ferrocyanide ($K_4Fe(CN)_6$) for 1.5 h. Next, the cells were washed with 1.5% uranyl acetate, dehydrated in a series of graded ethanol and then embedded in Poly/Bed 812 resin. The cells were sectioned using Reichert Jung Ultracut S (Leica, Wetzlar, Hessen, Germany), after which they were stained with uranyl acetate and lead citrate. The cells were then observed and photographed using a ZEISS EM 902A [22].

Total RNA preparation and isolation

Total RNA was extracted from the hMSC using either RNAzolB (Tel-Test Inc., Friendswood, TX, USA) [23,24] or a RNeasy mini kit (Qiagen Inc., Germantown, MD, USA). The RNA was eluted using RNase-free water (Jeil Biotechservices Inc., Daegu, Korea), after which the total RNA was purified, diluted and quantified using a BioPhotometer (Eppendorf, Hamburg, Germany). The integrity was assessed by agarose gel electrophoresis.

Microarray procedure and data analysis

Total RNA was isolated, labeled and prepared for hybridization to a microarray gene chip (Affymetrix, Santa Clara, CA, USA) following the manufacturer's instructions. Hybridization was then conducted overnight using 15 μg labeled RNA product, after which the arrays were scanned using Affymetrix scanners. The gene expression profile of the cells was created using the Affymetrix system (Beyond Bioinformatics ISTECH AATC Gyeonggi, South Korea) in conjunction with the Human U133 Plus 2.0 50 K microarray, which contains approximately 54 675 probes. Pre-treatment was conducted using the GCOS global scaling in GenPlex software (Istech Corp., Korea). Differences in the distribution of data were confirmed by comparing an MA plot of the control array to a plot of the experimental array.

Data were considered significantly different when the expression changed by at least two-fold at three consecutive time-points compared with the expression of the control (0 h). Increased gene expression also had to include at least one present call (Affymetrix algorithm) or both control points needed to be present when gene expression increased or decreased.

Semi-quantitative RT-PCR assays

Selected microarray results were confirmed by comparison with relative messenger (m) RNA levels obtained by semi-quantitative reverse transcription (RT)–polymerase chain reaction (PCR) using gene-specific primer pairs. cDNA was prepared using a Thermocycler T3000 PCR machine (Whatman Biometra, Goettingen, Niedersachsen, Germany). Next, total RNA (2 μg) was reverse-transcribed using the ImProm-II reverse transcription system (A3800; Promega, Madison, WI, USA) and oligo dT primers according to the manufacturer's instructions. The PCR reactions were conducted using 100 ng cDNA, 5 mm of each primer and Biomix (Biolines, Taunton, MA, USA) in 10-μL reactions. In addition, a control cDNA sample was taken from each gene to establish a standard curve. Each reaction was then subjected to melting point analysis to confirm that only a single product had been amplified. All reactions were run in triplicate and the mean averages determined. Each band amplified by RT-PCR was normalized against β-actin expression to remove relative quantitative template errors. The PCR products were then separated on 1% agarose gels, after which they were visualized by ethidium bromide staining. All bands in these experiments were calculated and normalized by densitometry using FUJI FILM Multi Gauge version 2.0. The results of the RT-PCR analysis were expressed as the percentage of gene expression in hMSC that were incubated for 12 h compared with hMSC that were incubated for 0 or 6 h. To determine the optimal conditions for the detection and quantitation of gene expression, the relative yield of the PCR products amplified following various numbers of cycles were compared (data not shown).

MTS cytotoxicity assay

hMSC incubated for 6 or 12 h in PBS were seeded at a density of 4×10^4 cells/well in flat-bottomed 96-well plates. After 3 days, the culture medium was replaced with fresh medium containing MTS tetrazolium reagent (Promega) according to the manufacturer's instructions. After the incubation for 4 h, cell viability was assessed by measuring the absorbance in an automated plate reader (Bio Tek Instruments, Winooski, Vermont, USA) at 490 nm wavelength.

Results

Analysis of cell viability by FACS

To determine the level of apoptosis and necrosis in response to incubation in PBS for various lengths of time, we labeled hMSC with Annexin V and PI, respectively, and then evaluated the samples by FACS analysis. Cells incubated in PBS for 3, 6 and 12 h showed a higher degree of apoptosis and necrosis than control cells (Figure 1), although the FACS data did indicate that control cells exhibited a low level of apoptosis. Specifically, the viability of the cells at each time-point was as follows: 0 h, 91.83%; 3 h, 86.25%; 6 h, 83.11%; 12 h, 76.36%.

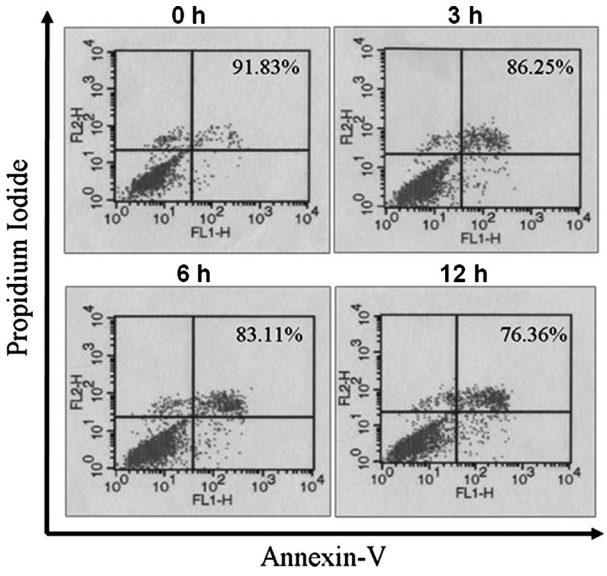

Figure 1. *hMSC were incubated for 0, 3, 6 and 12 h in PBS and then quantified by FACS analysis after staining with Annexin V/PI (Becton Dickinson Facsvantage). The viability of the cells decreased to 76% over time (0–12 h).*

Flow cytometry using 7-AAD cell-surface staining revealed a similar pattern, indicating that the cell viability decreased over time (data not shown).

Evaluation of the ultrastructural morphology of hMSC

Ultrathin sections of the cell suspensions were analyzed and photographed using TEM. Evaluations were conducted using 12 photographs per sample (×3000 magnification) taken in randomly chosen fields from several samples (Figure 2). Approximately 100 cells with visible nuclei were evaluated per suspension on blind-coded images and then divided into one of three categories according to the appearance of nuclear chromatin and membrane and the presence of cytosolic vacuoles, as described in a previous study [18]. Cells incubated for 0 (Figure 2a–c) and 3 h (Figure 2d–f) appeared to be healthy, with more than 80% cell membranes being clear and round and obvious nuclei being present. Approximately half of the cells in these groups also contained less than two or three cytosolic vacuoles. Conversely, the cytosol and vacuole state of cells that were incubated for 6 h (Figure 2g–i) was similar to that of cells that were incubated for 0 and 3 h but the membrane morphology was distorted. Cells that were incubated for 12 h (Figure 2j–l) appeared crushed and had more than 10 vacuoles. Additionally, the nucleoli in cells that were incubated for 12 h were not clearly detected. Finally, there was a high level of cell debris in samples that were incubated for 12 h compared with the other samples (data now shown).

Microarray analysis

To analyze changes in mRNA expression over time, we evaluated hMSC that were cultured for 0, 6 and 12 h in PBS using oligonucleotide microarrays. After appropriate background normalization, 2771 of 2949 functional genes were divided into six clusters using the GenPlex software (Figure 3).

Most of the up-regulated genes were related to the ubiquitin cycle, ion binding and apoptosis. In total, 921 genes were up-regulated at 6 and 12 h compared with the controls, with the expression of 904 genes and 527 genes being up-regulated after 6 and 12 h of treatment, respectively. Of these 921 up-regulated genes, 510 were up-regulated after incubation for both time periods (Table I). The genes in the up-regulated group included CREB5, RAB6A, BCLAF1, BCL2L13, PTPN13, NFRκB, TNFRSF8, TIFA, PLCB1, LONP, PEX13, TIFA and SERP1.

Most of the down-regulated genes were found to be involved in cell adhesion, DNA repair, development and oxidoreductase activity. Of the 1266 genes that were down-regulated, 841 and 739 were down-regulated after 6 and 12 h of treatment, respectively. In addition, of the 1266 down-regulated genes, 314 were common between the 6- and 12-h time-points (Table I). The important genes in the down-regulated group included CDH26, PCDH20, PELO, IKBKAP, ARHGEF9 and CASK.

We also categorized the genes that showed the greatest change in expression after 6 and 12 h of incubation. We found that genes that were involved in apoptosis and stress showed the greatest changes over time. The 25 genes that displayed the most significant changes after 6 and 12 h are listed in Table II.

Confirmation of gene expression by semi-quantitative RT-PCR

RT-PCR was performed to characterize better the genes involved in cell death that were differentially expressed after 6 and 12 h of treatment. Figure 4 shows the results of RT-PCR analysis of the up- and down-regulated genes. Several of these genes were found to contribute to the cAMP-responsive element binding protein 5 (CREB5). In addition, several cell death signal-related factors were

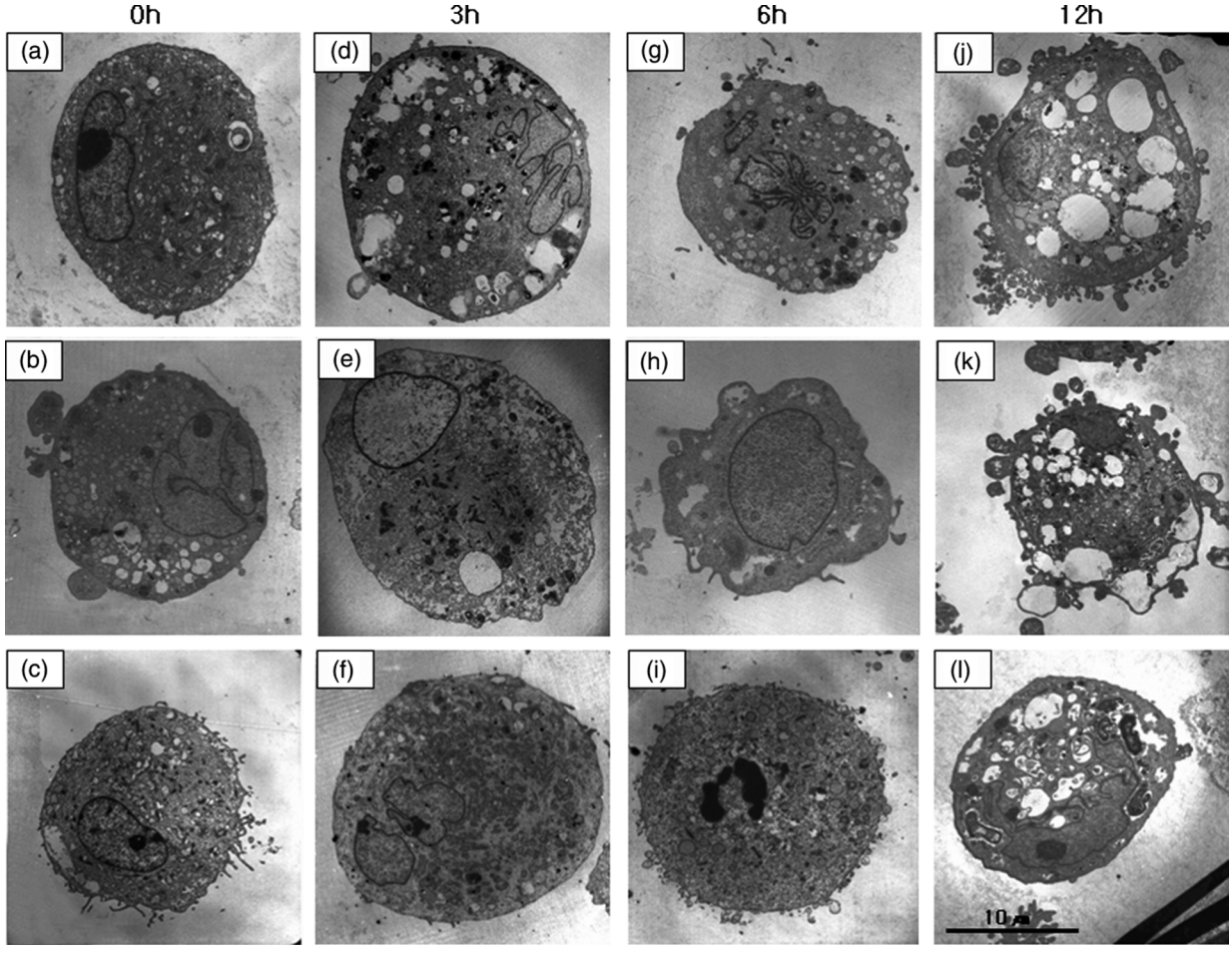

Figure 2. *TEM (×3000 original magnification) of hMSC. Cells were incubated in PBS at room temperature for 0–12 h. Visible nuclei were then evaluated, after which cells were divided into two categories based on the appearance of the membrane and presence of cytosolic vacuoles. Cells that were incubated for 0 (a–c) and 3 h (d–f) appeared to be healthy, as indicated by most cell membranes being round and clear and the nuclei of these groups being easily identified. In addition, some of these cells contained a few cytosolic vacuoles. The cytosol and vacuole state of cells that were incubated for 6 h (g–i) were similar to those of cells that were incubated for 0 and 3h, but the membrane morphology was distorted. Cells that were incubated for 12 h (j–l) appeared to be crushed and contained large vacuoles.*

up-regulated, including BCL2-associated transcription factor 1 (BCLAF1) and the apoptosis facilitator BCL2-like 13 (BCL2L13). Moreover, a member of the RAS oncogene family (RAB6A), TRAF-interacting protein with a forkhead-associated domain (TIFA) and peroxisomal ion protease (LONP) were down-regulated after 12 h of treatment. Furthermore, human pelota gene (PELO) and calcium/calmodulin-dependent serine protein kinase (CASK) were down-regulated. Consequently, we confirmed that the expression level of genes related to apoptosis and stress, such as CREB5, RAB6A, BCLAF1, BCL2L13, TIFA, LONP, PELO and CASK, changed significantly over time. Taken together, these results demonstrated that genes related to apoptosis, signal transduction, cell death, growth factor, cell adhesion and oxidative stress were differentially expressed over time after incubation in PBS. These findings indicate that a better understanding of the conditions that lead to dissociation of hMSC may enable development of more efficient therapeutic strategies.

Evaluation of cell viability after incubation

We performed an MTS assay to evaluate the reversible viability of hMSC incubated for 6 or 12 h. There was a

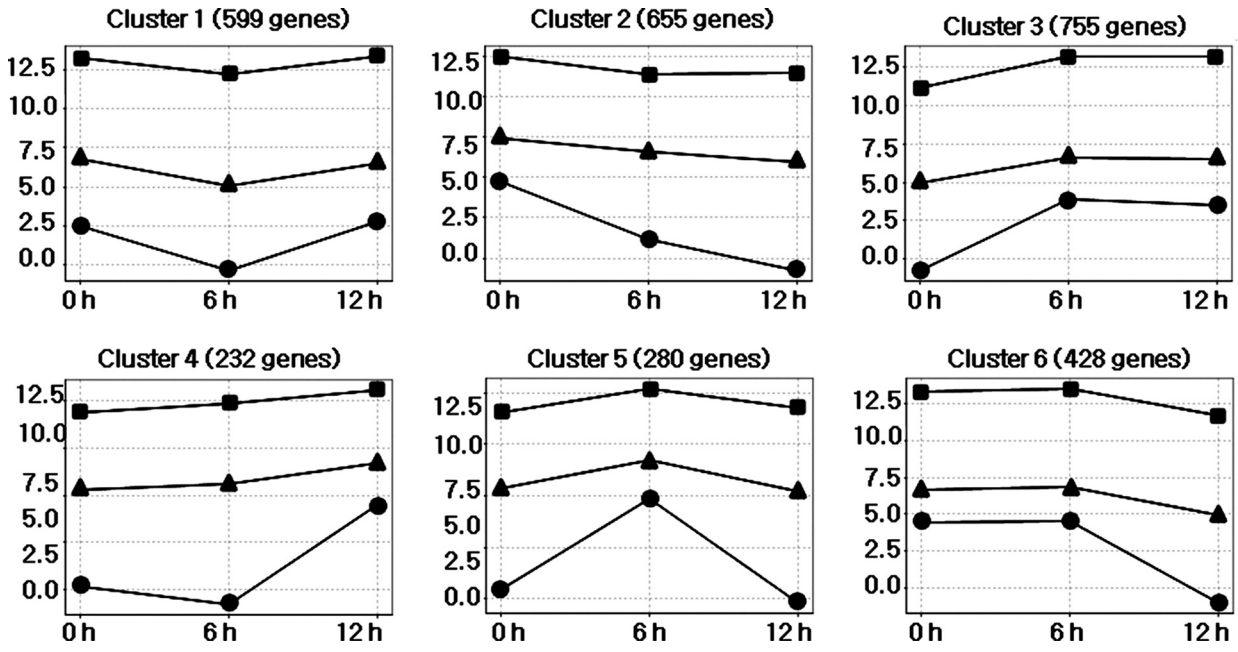

Figure 3. *Clustering of gene expression in hMSC after incubation for different lengths of time (0, 6 and 12 h); 2771 genes were selected based on the fold change in expression (cut-off ≥ 2). The dendrogram produced showed six clusters using the Genplex software and the expression levels of genes in each cluster are shown as graphs (squares, maximum; triangles, average; circles, minimum).*

significant reduction of proliferation activity between 0 and 12 h ($P<0.001$) but no significant difference between 0 and 6 h (Figure 5). Thus, for reversible viability, hMSC should be applied within 6 h of dissociation.

Discussion

We used FACS and microarray analysis to evaluate the viability and gene expression profile of hMSC over time. The results of these analyzes revealed that time is a critical factor that may impact the clinical application of hMSC.

FACS analysis revealed that 83% and 76% of cells were viable after 6 and 12 h of incubation, respectively. This suggests that with increasing time in PBS, cells became more sensitive to any treatment or manipulation, such as preparation for FACS. However, when cell viability was evaluated using the trypan blue (TB) exclusion test, more than 97.8% of the cells were viable at 0 h, and 94.4%, 93.4% and 89.8% of the cells were found to be viable after storage at room temperature for 3, 6 and 12 h, respectively (data not shown). However, the TB data do not quite go hand in hand with the FACS results. The value of 89.8% viable cells (TB staining) after 12 h in PBS is very high and essentially not detrimental in a therapeutic context. Although TB cell counting is normally

Table I. Data mining by expression level ratio.

		Up-regulated genes		Down-regulated genes	
Total probes	Filtered genes	Time (h)	Fold change ≥ 2	Time (h)	Fold change ≥ 2
54765	2771	0–6	904	0–6	841
		6–12	527	6–12	739
		0–12	868	0–12	1098
		0–6	40	0–6	52
		6–12		6–12	
		0–6	510	0–6	314
		0–12		0–12	

Genes that were increased or decreased by twice the cut-off value were selected for further analysis.

Table II. Twenty-five genes selected by data mining based on the expression level ratio. Criteria are the same as those described for Table I.

Full name	Symbol	0 h signal	6 h signal	12 h signal	Cluster	Chromosome location	UniGene ID	Primer sequence (sense/antisense)
Phosphodiesterase 4D, cAMP-specific (phosphodiesterase E3 dunce homolog, Drosophila)	PDE4D	10.9	90.7	121.2	3	chr5q12	Hs.117545	GCACTGATTTACAAGACATCG
								CATAGACCAGAGACCATTATTTGAG
cAMP-responsive element binding protein 5	CREB5	10.9	63.5	94.9	3	chr7p15.1	Hs.437075	CACACATTCAGGACACCAG
								AGATTTATTAACTAGACCCCAGG
RAB6A, member of RAS oncogene family	RAB6A	2.5	62.3	7.1	5	chr11q13.3	Hs.535586	GATGAAAAGCCAGGTGAAGG
								CCTGGCCCAAATTCTTTTTTT
BCL2-associated transcription factor 1	BCLAF1	32.2	73.9	93.4	3	chr6q22-q23	Hs.486542	TTGCTTACTTGGGATTGAGAAGAA
								TTCTAACACCTTGCAATTCCCAT
BCL2-like 13 (apoptosis facilitator)	BCL2L13	53.5	377.7	270.7	3	chr22q11	Hs.546359	CAGGGTAGGTAAAGTATTTTTAT
								CCTAAAGGAAGGGTAGAC
Protein tyrosine phosphatase, non-receptor type 13 [APO-1/CD95 (Fas)-associated phosphatase]	PTPN13	10	57.4	72.9	3	chr4q21.3	Hs.436142	GAGGAGACATCTCCTTGATCTAGG
								TATGCTATAGTGCTGTGCTATCACC
Nuclear factor related to kappaB binding protein	NFRKB	29.9	77	60.1	3	chr11q24-q25	Hs.530539	GCAGCTAAAGCCCAAGTTTG
								TCCATGAGGATTGTATTTTTTGG
Tumor necrosis factor receptor superfamily, member 8	TNFRSF8	57.2	127.7	209.1	3	chr1p36	Hs.1314	GAGGCTCCAGCATCTAGTGG
								AATGCTGTTCTCGGCAGTG
TRAF-interacting protein with a forkhead-associated domain	TIFA	2.3	36.2	67.8	3	chr4q25	Hs.310640	TTAAACATTTTAAAGAACACTGTG
								GATACTATTAAGAAGGTGAATTCG
Phospholipase C, beta 1 (phosphoinositide-specific)	PLCB1	38.6	106.7	93	3	chr20p12	Hs.310537	GGCCAGGCTAAGATTCAAATTC
								AGAGGGTCATTTCCTATGCTGC
Peroxisomal lon protease	LONP	7.6	52.1	57.3	3	chr16q12.1	Hs.551565	CTAGGTCGAGAGTTCCACAG
								GTTGTTCACTCCCACAGTCT
Peroxisome biogenesis factor 13	PEX13	61.8	205.4	164.7	3	chr2p14-p16	Hs.336219	GAATCAAGTAAAGTTTCCAAG
								ATAAATTTCAGACTTTTTGCT

Table II. *(Continued).*

Full name	Symbol	0 h signal	6 h signal	12 h signal	Cluster	Chromosome location	UniGene ID	Primer sequence (sense/antisense)
Stress-associated endoplasmic reticulum protein 1	SERP1	11.1	67.7	57.1	3	chr3q25.1	Hs.518326	CAACTGGCAAAGGGAGATCA
								TGCAGAGGCACAGTGTAAGG
Brain-derived neurotrophic factor opposite strand	BDNFOS	119.8	59.9	23.6	2	chr11p14.1	—	TAGATGATGATGGCACAAAA
								GTTGGTGCAGGTATCAGATT
Signal peptide, CUB domain, EGF-like 3	SCUBE3	71	223.4	32.9	5	chr6p21.3	Hs.12923	CGAATCTGAAATGAGTTTATTTTTT
								TAGTGAAGTGGGGGAAGAACA
Cadherin-like 26	CDH26	35.5	71.9	5.8	6	chr20q13.2-q13.33	Hs.54973	CTACCTACCTCACGTCTACAG
								TATAAAGCTTTCAGCATAATC
Protocadherin 20	PCDH20	53.6	46	8.2	6	chr13q21	Hs.391781	GACAGGCACTTCAGTGAAAT
								TCTGTACTGTACCAAAAGTG
Integrin, alpha 1	PELO	69.6	69.2	30.1	6	chr5q11.2	Hs.519304	CATGAAGCTCGTGAGGAAGAACAT CGAG
								GCAGATATGGGCGAGGCCTTC
Inhibitor of kappa light polypeptide gene enhancer in B-cells, kinase complex-associated protein	IKBKAP	86.1	100.2	42.5	6	chr9q31	Hs.494738	GCTTTAGTTTAAGGTGACAAGAAGC
								CAAAGTGTGAAGACAAGTAAAACAA
Cell division cycle 2-like 5 (choline-|sterase-related cell division controller)	CDC2L5	136.7	88.1	31	2	chr7p13	Hs.233552	GGCTCCTTGGACGACTTAGT
								GGTCTCCAAGTCCCGCAG
CDC42-binding protein kinase alpha (DMPK-like)	CDC42BPA	233.5	168.3	61.8	2	chr1q42.11	Hs.35433	GATCAAAATAATAACCCTACCTA
								CCTAGACAAGCCTCAGTA
Cdc42 guanine nucleotide exchange factor (GEF) 9	ARHGEF9	207.2	242.7	89.2	6	chrXq11.2	Hs.54697	CCATAAATATTTTCATAAGGCTTTG
								GGTGGATGGATGGGCAAC
Calcium/calmodulin-dependent serine protein kinase (MAGUK family)	CASK	182.1	110.3	7.4	6	chrXp11.4	Hs.495984	GGCTCACTAACTCACATCTGG
								GGGGATGAATCTCAATACCA
Orphan short-chain dehydrogenase/ reductase	SDR-O	9.8	52.5	3.6	5	chr12q13.3	Hs.380178	AGGATGACTTTGTGAAGGTG
								AGTAGAGCTCACGCCTTATG
Peroxiredoxin 3	PRDX3	77.5	146.2	7.4	6	chr10q25-q26	Hs.523302	AAGATGGTTATTTGTAGAAGG
								ACAGTTACTTGGTGGTAAAAT

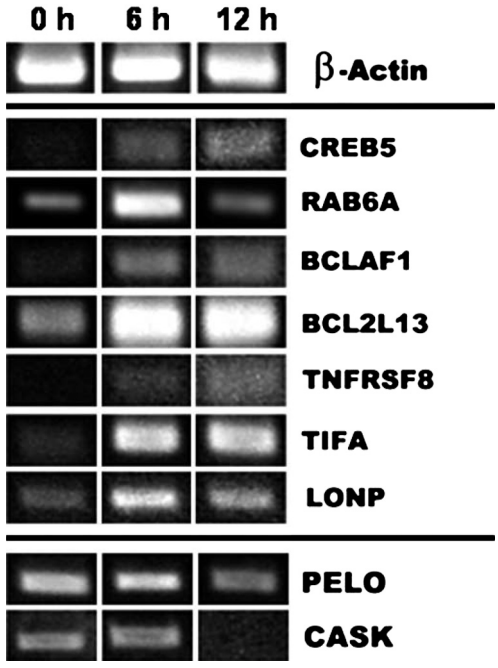

Figure 4. *Semi-quantitative RT-PCR analysis of the selected differentially expressed genes. The band intensities were calculated by densitometry after normalization against the β-actin gene. Up- and down-regulated genes were then confirmed by RT-PCR.*

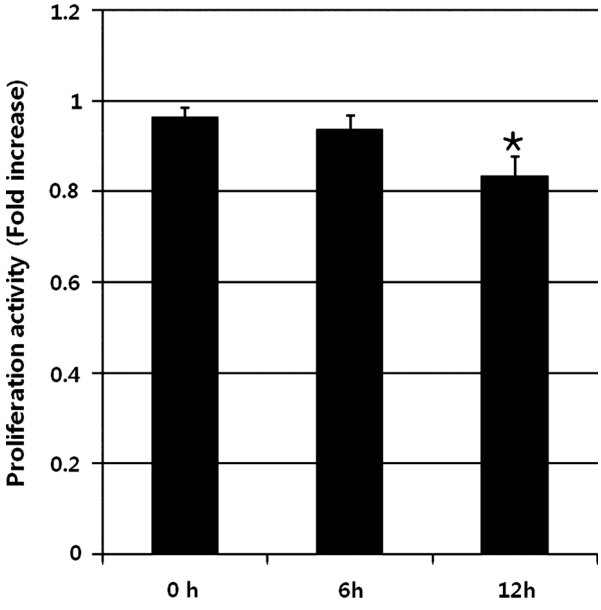

Figure 5. The cell viability of hMSC measured by MTS assay after incubation in PBS. Proliferation activity is indicated as fold change relative to 0 h. *A significant change was observed ($P < 0.001$).

applied to cell viability assay because of its simplicity and convenience, there is the possibility of subjective evaluation. Therefore, evaluation using both FACS and TB data could lead to appropriate viability assessment in a clinical setting to ensure cell viability.

The results of this study indicate that some protective measures may be induced to counteract the effects of cellular damage after disassociation from the culture dish. Gordon *et al.* 25] demonstrated that the use of 50 mm trehalose, a disaccharide that has been identified in organisms capable of withstanding desiccation, could act as a protective agent for hMSC during transport. Therefore, it is possible that reagents that protect against cell death can be used to increase the efficiency of stem cell transplantation during cell therapy.

In the present study, we focused on the viability of hMSC over time. Further clarifications on the proliferation capacity, immunogenicity and differentiation potential of the incubated hMSC *in vivo* remained to be solved. Additional studies on the potential consequences of these changes in therapeutic efficiency will be necessary for the development of appropriate therapeutic strategies in the future.

The survival of hMSC is critical for clinical applications as their viability effectively determines the outcome of treatment. However, the effects of standard cell culture techniques on hMSC are not well understood. In this study, we have demonstrated that the preparation of hMSC for clinical applications such as cell therapy should be conducted as quickly and efficiently as possible, while taking care not to cause any stress to the cells.

Overall, the results of this study indicate that time is an important factor that must be considered during stem cell-based therapy; therefore, hMSC should be used as soon as possible following dissociation from the culture dish.

Acknowledgements

This work was supported by the Korea Research Foundation Grant funded by the Korean Government (MOEHRD, Basic Research Promotion Fund; KRF-2007-313-H00012) to Gwang Lee, and partly supported by a Korea Science and Engineering Foundation (KOSEF) grant funded by the Korean Government (MOST; R01-2007-000-20533–0) to Sangdun Choi.

Declaration of interest: The authors report no conflicts of interest. The authors alone are responsible for the content and writing of the paper.

References

1. Bang OY, Lee JS, Lee PH, Lee G. Autologous mesenchymal stem cell transplantation in stroke patients. *Ann Neurol* 2005;57:874–82.
2. Tse HF, Kwong YL, Chan JK, Lo G, Ho CL, Lau CP. Angiogenesis in ischaemic myocardium by intramyocardial autologous bone marrow mononuclear cell implantation. *Lancet* 2003;361:47–9.
3. Tateishi-Yuyama E, Matsubara H, Murohara T, Ikeda U, Shintani S, Masaki H, *et al.* Therapeutic angiogenesis for patients with limb ischaemia by autologous transplantation of bone-marrow cells: a pilot study and a randomised controlled trial. *Lancet* 2002;360:427–35.
4. Lee PH, Kim JW, Bang OY, Ahn YH, Joo IS, Huh K. Autologous mesenchymal stem cell therapy delays the progression of neurological deficits in patients with multiple system atrophy. *Clin Pharmacol Ther* 2008;83:723–30.
5. Friedenstein AJ, Deriglasova UF, Kulagina NN, Panasuk AF, Rudakowa SF, Luriá EA, *et al.* Precursors for fibroblasts in different populations of hematopoietic cells as detected by the in vitro colony assay method. *Exp Hematol* 1974;2:83–92.
6. Pittenger MF, Mackay AM, Beck SC, Jaiswal RK, Douglas R, Mosca JD, *et al.* Multilineage potential of adult human mesenchymal stem cells. *Science* 1999;284:143–7.
7. Frankel MS. In search of stem cell policy. *Science* 2000;287: 1397.
8. Ballas CB, Zielske SP, Gerson SL, Adult bone marrow stem cells for cell and gene therapies: implications for greater use. *J Cell Biochem* 2002;38 Suppl:20–8.
9. Mackay AM, Beck SC, Murphy JM, Barry FP, Chichester CO, Pittenger MF. Chondrogenic differentiation of cultured human mesenchymal stem cells from marrow. *Tissue Eng* 1998;4:415–28.
10. Schultz SS, Lucas PA. Human stem cells isolated from adult skeletal muscle differentiate into neural phenotypes. *J Neurosci Methods* 2006;152:144–55.
11. Sekiya I, Larson BL, Vuoristo JT, Cui JG, Prockop DJ. Adipogenic differentiation of human adult stem cells from bone marrow stroma (MSCs). *J Bone Miner Res* 2004;19:256–64.
12. Gregory CA, Prockop DJ, Spees JL. Non-hematopoietic bone marrow stem cells: molecular control of expansion and differentiation. *Exp Cell Res* 2005;306:330–5.
13. George J, Kuboki Y, Miyata T. Differentiation of mesenchymal stem cells into osteoblasts on honeycomb collagen scaffolds. *Biotechnol Bioeng* 2006;95:404–11.
14. Cheng L, Qasba P, Vanguri P, Thiede MA. Human mesenchymal stem cells support megakaryocyte and pro-platelet formation from CD34(+) hematopoietic progenitor cells. *J Cell Physiol* 2000;184:58–69.
15. Abdallah BM, Kassem M. Human mesenchymal stem cells: from basic biology to clinical applications. *Gene Ther* 2008;15:109–16.
16. Lindvall O, Kokaia Z, Martinez-Serrano A. Stem cell therapy for human neurodegenerative disorders: how to make it work. *Nat Med* 2004;10 Suppl:S42–50.
17. Li Y, Chen J, Chen XG, Wang L, Gautam SC, Xu YX, *et al.* Human marrow stromal cell therapy for stroke in rat: neurotrophins and functional recovery. *Neurology* 2002;59: 514–23.
18. Ahn YH, Emgard M, Brundin P. Ultrastructural characterization of dissociated embryonic ventral mesencephalic tissue treated with neuroprotectants. *Cell Transplant* 2003;12: 235–41.
19. Brundin P, Karlsson J, Emgard M, Schierle GS, Hansson O, Petersén A, *et al.* Improving the survival of grafted dopaminergic neurons: a review over current approaches. *Cell Transplant* 2000;9:179–95.
20. Abranches E, Bekman E, Henrique D, Cabral JM. Expansion and neural differentiation of embryonic stem cells in adherent and suspension cultures. *Biotechnol Lett* 2003;25: 725–30.
21. De Ugarte DA, Morizono K, Elbarbary A, Alfonso Z, Zuk PA, Zhu M, *et al.* Comparison of multi-lineage cells from human adipose tissue and bone marrow. *Cells Tissues Organs* 2003;174:101–9.
22. Kim SH, Won SJ, Sohn S, Kwoh HJ, Lee JY, Park JH, *et al.* Brain-derived neurotrophic factor can act as a pronecrotic factor through transcriptional and translational activation of NADPH oxidase. *J Cell Biol* 2002;159:821–31.
23. Chomczynski P, Sacchi N. Single-step method of RNA isolation by acid guanidinium thiocyanate-phenol-chloroform extraction. *Anal Biochem* 1987;162:156–9.
24. Siebert PD, Chenchik A. Modified acid guanidinium thiocyanate-phenol-chloroform RNA extraction method which greatly reduces DNA contamination. *Nucleic Acids Res* 1993;21:2019–20.
25. Gordon SL, Oppenheimer SR, Mackay AM, Brunnabend J, Puhlev I, Levine F.. Recovery of human mesenchymal stem cells following dehydration and rehydration. *Cryobiology* 2001;43:182–7.